Journal of Molecular Liquids 209 (2015) 625–634

Contents lists available at ScienceDirect

Journal of Molecular Liquids

journal homepage: www.elsevier.com/locate/molliq

Geometrical structure, molecular docking, potentiometric and thermodynamic studies of 3-aminophenol azodye and its metal complexes

A.Z. El-Sonbati [a,*], G.G. Mohamed [b], A.A. El-Bindary [a], W.M.I. Hassan [b], A.K. Elkholy [a,1]

[a] Chemistry Department, Faculty of Science, Damietta University, Damietta 34517, Egypt
[b] Chemistry Department, Faculty of Science, Cairo University, Giza 12613, Egypt

ARTICLE INFO

Article history:
Received 14 April 2015
Received in revised form 31 May 2015
Accepted 2 June 2015
Available online xxxx

Keywords:
3-Aminophenol azodye
Potentiometry study
Stability constants
Thermodynamics parameters
Quantum chemical parameters
Molecular docking

ABSTRACT

The proton–ligand dissociation constants of 4-(2,3-dimethyl-1-phenylpyrazol-5-one azo)-3-aminophenol (HL) and its metal stability constants with Mn(II), Co(II), Ni(II) and Cu(II) ions have been determined using potentiometric studies. The molecular structure of the ligand is optimized theoretically and the quantum chemical parameters are calculated. The proton–ligand dissociation constants of HL and its metal stability constants with Mn(II), Co(II), Ni(II) and Cu(II) have been determined potentiometrically. The potentiometric studies were carried out in 0.1 M KCl and 20% (by volume) DMF–water mixture. At constant temperature the stability constants of the formed complexes decrease in the order of Cu(II) > Ni(II) > Co(II) > Mn(II). The effect of temperature was studied at 298, 308 and 318 K and the corresponding thermodynamic parameters (ΔG, ΔH and ΔS) were derived and discussed. The dissociation process is non-spontaneous, endothermic and entropically unfavorable. The formation of the metal complexes has been found to be spontaneous, endothermic and entropically favorable. Molecular docking was used to predict the binding between azodye ligand and the receptor of prostate cancer mutant 2q2k-Hormon and receptor of breast cancer mutant 3hb5-Oxidoreductase.

1. Introduction

Azo compounds containing heterocyclic moieties have drawn the attention of many researchers [1–5]. It has been well established that the use of heterocyclic amines with oxygen as the π-excessive hetero atom as diazo component has a marked bathochromic effect compared to analogous dyes derived from benzenoid compounds [6]. Azo derivatives containing antipyrine moiety have many advantages including color depending effect as an intrinsic property leading to better dye ability. The color of these azo derivatives depends on the nature of both the diazo and the coupling components. Majority of the azo compounds are derived from the coupling of diazotized heterocyclic amines with aromatic hydroxyl and amino compounds. The position of azo and hydroxyl groups in these molecules brings into play the azo-hydrazone equilibrium [7]. The use of protein–ligand docking has become a standard method in potentiometric studies. The protein groups surrounding the ligand can highly influence the local pH, so that a different protonation could be favored in the bound state. To account for this effect, the ideal case would be to use multiple protonations in the docking and have the algorithm automatically pick the correct state. Molecular docking is widely used to predict protein–ligand [8,9] and to screen large libraries for molecules that will modulate the activity of a biological receptor.

In this paper, the potentiometric studies are used to determine the dissociation constants of 4-(2,3-dimethyl-1-phenylpyrazol-5-one azo)-3-aminophenol ligand (HL) and the stability constants of its complexes with some divalent transition metal ions such as Mn(II), Co(II), Ni(II) and Cu(II) at different temperatures. The molecular structure of the investigated ligand (HL) is studied and quantum chemical parameters are calculated. Moreover, the corresponding thermodynamic functions are calculated and discussed.

2. Materials and methods

2.1. Preparation of the ligand

4-(2,3-Dimethyl-1-phenylpyrazol-5-one azo)-3-aminophenol ligand (HL) was prepared previously [2–5,10] by coupling an equimolar amount of 1-phenyl-2,3-dimethyl-4-amino pyrazol-5-one and 3-aminophenol as shown in Scheme 1. In a typical preparation, 25 ml of distilled water containing 0.01 mol hydrochloric acid was added to 1-phenyl-2,3-dimethyl-4-amino pyrazol-5-one (0.01 mol). To the resulting mixture stirred and cooled to 0 °C, a solution of 0.01 mol sodium nitrite in 20 ml of water was added dropwise. The formed diazonium chloride was consecutively coupled with an alkaline solution of

* Corresponding author.
E-mail address: elsonbatisch@yahoo.com (A.Z. El-Sonbati).
[1] Abstracted from her Ph.D. Thesis.

http://dx.doi.org/10.1016/j.molliq.2015.06.010
0167-7322/

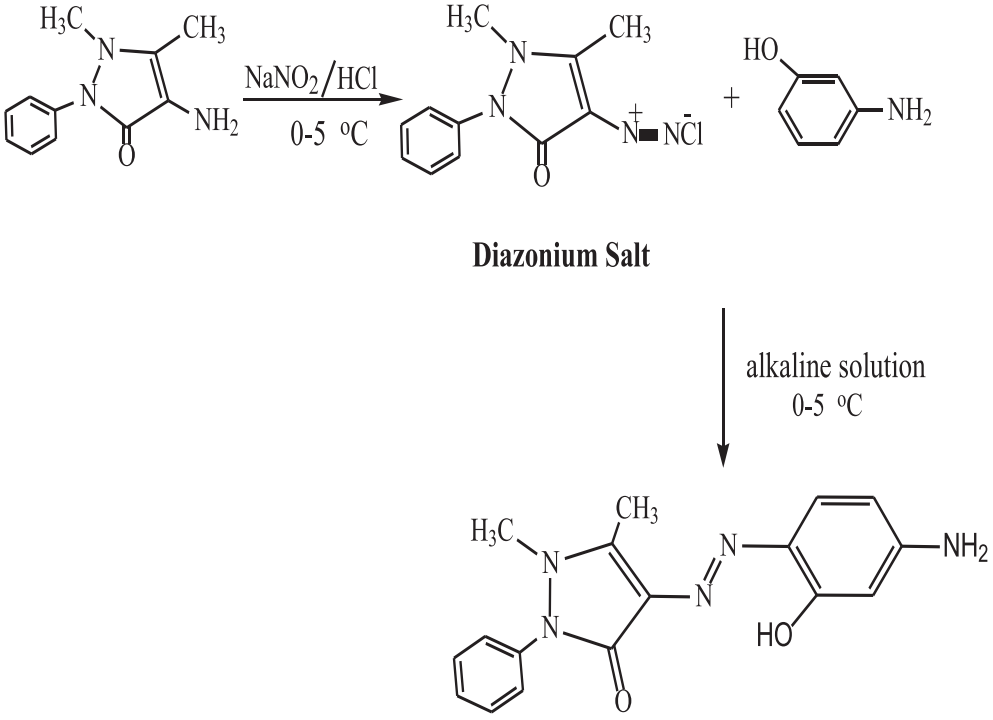

Scheme 1. The formation mechanism of the azo ligand (HL).

0.01 mol 3-aminophenol, in 10 ml of pyridine. Immediately, the deep purple precipitate formed was filtered through sintered glass crucible, washed several times by distilled water. The crude product was purified by recrystallization from hot ethanol, (yield ~68%) then dried in a vacuum desiccator over anhydrous P_2O_5. The structure of the formed ligand (HL) was established by IR, ^{1}H NMR and X-ray spectroscopies.

2.2. Potentiometric studies

A ligand solution (0.01 M) was prepared by dissolving an accurately weighed amount of the solid in DMF. Metal ion solutions (0.001 M) were prepared from metal chloride salts in bidistilled water and standardized with EDTA [11]. Solutions of 0.005 M HCl and 1 M KCl were

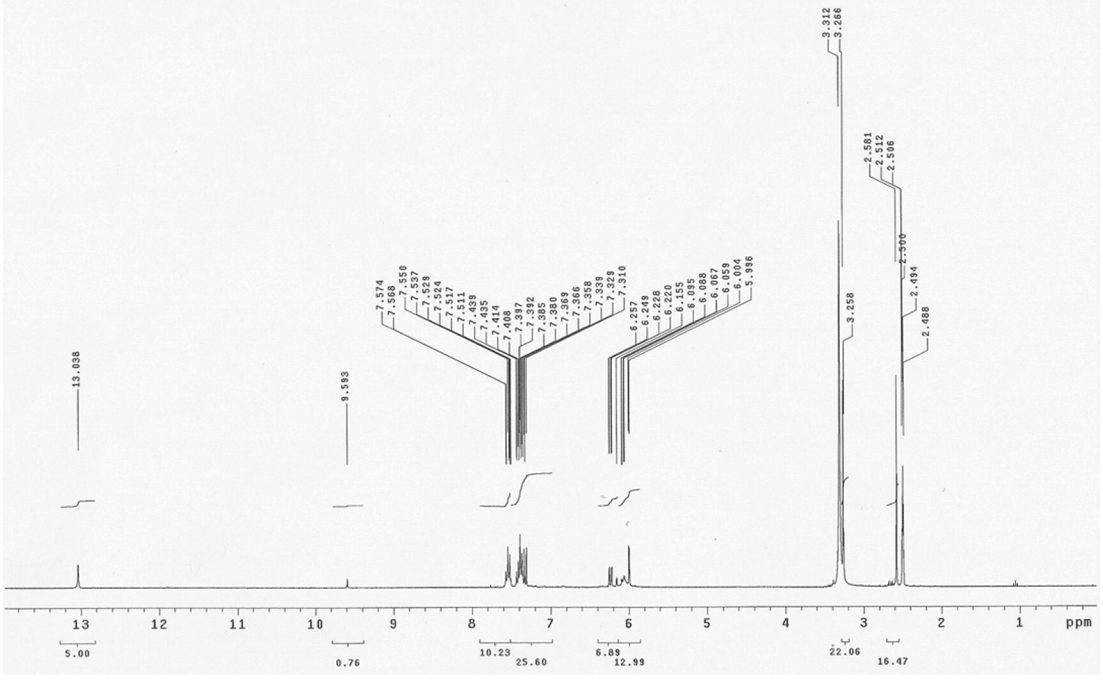

Fig. 1. ^{1}H NMR spectrum of HL ligand

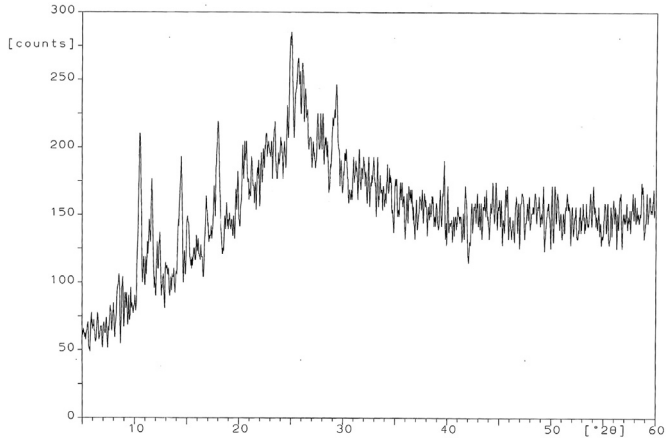

Fig. 2. X-ray diffraction pattern of HL powder form.

also prepared in bidistilled water. A carbonate-free NaOH solution in 20% (by volume) DMF–water mixture was used as titrant and standardized against oxalic acid.

The apparatus, general conditions and methods of calculation were the same as in the previous work [2,3,12–15]. The following mixtures (i)–(iii) were prepared and titrated potentiometrically at 298 K against standard 0.02 M NaOH in a 20% (by volume) DMF–water mixture:

i) 5 cm^3 0.005 M HCl + 5 cm^3 1 M KCl + 10 cm^3 DMF.
ii) 5 cm^3 0.005 M HCl + 5 cm^3 1 M KCl + 5 cm^3 0.01 M ligand + 5 cm^3 DMF.
iii) 5 cm^3 0.005 M HCl + 5 cm^3 l M KCl + 5 cm^3 0.01 M ligand + 10 cm^3 0.001 M metal chloride + 5 cm^3 DMF.

For each mixture, the volume was made up to 50 cm^3 with bidistilled water before the titration. These titrations were repeated for the temperatures of 308 and 318 K. All titrations have been carried out between pH 3.0–12.0 and under nitrogen atmosphere.

2.3. Measurements

All the compounds and solvents used were purchased from Aldrich and Sigma and used as received without further purification. The IR spectra were recorded as KBr discs using a Perkin-Elmer 1340 spectrophotometer. The ^1H NMR spectrum was obtained with a JEOL FX90 Fourier transform spectrometer with DMSO-d_6 as the solvent and TMS as an internal reference. X-ray diffraction analysis of the ligand (HL) powder form was recorded on an X-ray diffractometer in the range of diffraction angle $2\theta^\circ = 5–60^\circ$. This analysis was carried out using CuKα radiation (λ = 1.54056 Å). The applied voltage and the tube current are 40 kV and 25 mA, respectively.

The molecular structure of the investigated compound was optimized initially with the PM3 semiempirical method so as to speed up the calculations. The resulting optimized structures were fully re-optimized using ab initio Hartree–Fock (HF) [16] with 6-31G basis set. The molecules were built with the Gauss View 3.09 and optimized using Gaussian 03W program [17]. The corresponding geometries were optimized without any geometry constraints for full geometry optimizations. Frequency calculation was executed successfully, and no imaginary frequency was found, indicating minimal energy structures.

In the study simulates the actual docking process in which the ligand-protein interaction energies are calculated using a Docking Server [18]. The MMFF94 Force field was for used energy minimization of ligand molecule using a Docking Server. Gasteiger partial charges were added to the ligand atoms. Non-polar hydrogen atoms were merged, and rotatable bonds were defined. Docking calculations were carried out on 2q2k-Hormone and 3hb5-Oxidoreductase protein models. Essential hydrogen atoms, Kollman united atom type charges, and solvation parameters were added with the aid of AutoDock tools [19]. Affinity (grid) maps of ×× Å grid points and 0.375 Å spacing were generated using the Autogrid program [20]. Auto Dock parameter set- and distance-dependent dielectric functions were used in the calculation of the van der Waals and the electrostatic terms, respectively.

The pH measurements were carried out using a VWR Scientific Instruments Model 8000 pH-meter accurate to ±0.01 units. The pH-meter readings in the non-aqueous medium were corrected [21]. The electrode system was calibrated according to the method of Irving et al. [22]. Titrations were performed in a double walled glass cell in an inert atmosphere (nitrogen) at an ionic strength of 0.1 M KCl. Potentiometric measurements were carried out at different temperatures. The temperature was controlled to within ±0.05 K by circulating thermostated water (Neslab 2 RTE 220) through the outer jacket of the vessel.

3. Results and discussion

3.1. Characterization of the ligand (HL)

3.1.1. IR spectra

The infrared spectrum of HL ligand gives interesting results and conclusions. The ligand gives a broad absorption band located at 3210 cm^{-1} assigned to υ(OH). The strong band at 1620 cm^{-1} is due to carbonyl stretching vibration mode. The frequency for the N═N stretching vibration was located at 1490 cm^{-1}. The region between 1219 and 1323 cm^{-1} is due C–OH stretching, C–OH in plane or out of plane bending and out-of-plane C–OH bending vibrations.

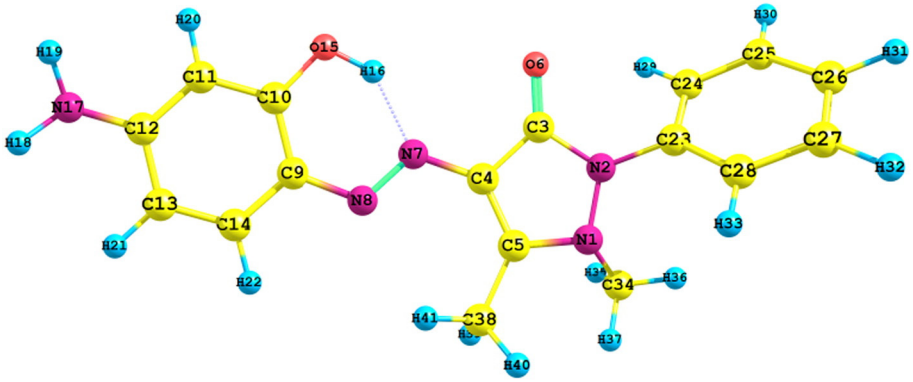

Fig. 3. The optimized structure of HL ligand within numbering of atoms.

3.1.2. ^{1}H NMR spectra

The ^{1}H NMR spectrum of the ligand was recorded in DMSO-d_6 at room temperature which supports the occurrence of the form depicted in Fig. 1. The =C–CH_3 and–N–CH_3 protons were observed as singlet at δ 2.47 and 2.60 ppm, respectively. In the aromatic region, a few doublets and in few cases some overlapping doublets/multiplets are observed in the range of δ 6.10–7.6 ppm. Another singlet corresponding to one proton for compound is observed in the range of δ ~9.59 and 13.03 ppm. This signal disappeared when a D_2O exchange experiment was carried out. It can be assigned to OH and NH (Scheme 1). The absence of –CH (3.85 ppm) proton signal of the ligand (HL) moiety indicated the existence of the ligand in the azo-enol form. According to El-Sonbati et al. [10], hydrogen bonding leads to a large deshielding of the protons.

3.1.3. X-ray diffraction

The X-ray diffraction, XRD, and pattern of the ligand (HL) is shown in Fig. 2. The XRD pattern of the ligand (HL) has sharp diffraction peaks at around 2θ = 10–20° and 2θ = 25–30°. This indicates that HL is a mixture of crystalline and amorphous phases.

3.2. Geometrical structure

Geometrical structures and electronic properties of the investigated compounds and their protonated forms were calculated by optimizing their bond lengths, bond angles and dihedral angles. The optimized structure of the HL ligand is presented in Fig. 3. Selected geometric parameters bond lengths and bond angles of HL ligand are tabulated in Tables 1 and 2. The HOMO and LUMO are shown in Fig. 4. Quantum chemical parameters of the ligand are obtained from calculations such as energies of the highest occupied molecular orbital (E_{HOMO}) and the lowest unoccupied molecular orbital (E_{LUMO}) as listed in Table 3. Additional parameters such as HOMO–LUMO energy gap, ΔE, absolute electronegativities, χ, chemical potentials, Pi, absolute hardness, η, absolute softness, σ, global electrophilicity, ω, global softness, S, and additional electronic charge, ΔN_{max} are calculated using the following Eqs. (1)–(8) [3,10,12]:

$$\Delta E = E_{LUMO} - E_{HOMO} \tag{1}$$

$$\chi = \frac{-(E_{HOMO} + E_{LUMO})}{2} \tag{2}$$

$$\eta = \frac{E_{LUMO} - E_{HOMO}}{2} \tag{3}$$

$$\sigma = \frac{1}{\eta} \tag{4}$$

$$Pi = -\chi \tag{5}$$

$$S = \frac{1}{2\eta} \tag{6}$$

Table 1
Selected geometric bond lengths of the ligand (HL).

Bond lengths (Å)	
R(N1,N2)	1.4107
R(N1,C5)	1.3869
R(N1,C34)	1.4702
R(N2,C3)	1.4168
R(N2,C23)	1.421
R(C3,C4)	1.4659
R(C3,O6)	1.2151
R(C4,C5)	1.3742
R(C4,N7)	1.3845
R(C5,C38)	1.4919
R(N7,N8)	1.275
R(N8,C9)	1.3843
R(C9,C10)	1.4306
R(C9,C14)	1.4094
R(C10,C11)	1.3935
R(C10,O15)	1.3366
R(C11,C12)	1.3978
R(C11,H20)	1.0843
R(C12,C13)	1.4148
R(C12,N17)	1.3826
R(C13,C14)	1.3761
R(C13,H21)	1.0841
R(C14,H22)	1.0839
R(O15,H16)	0.9948
R(N17,H18)	1.0077
R(N17,H19)	1.0079
R(C23,C24)	1.3984
R(C23,C28)	1.3985
R(C24,C25)	1.3915
R(C24,H29)	1.0809
R(C25,C26)	1.3945
R(C25,H30)	1.084
R(C26,C27)	1.3933
R(C26,H31)	1.0838
R(C27,C28)	1.3929
R(C27,H32)	1.0842
R(C28,H33)	1.0829
R(C34,H35)	1.096
R(C34,H36)	1.0886
R(C34,H37)	1.0884
R(C38,H39)	1.0961
R(C38,H40)	1.0923
R(C38,H41)	1.0875

Table 2
Selected geometric bond angles of the ligand (HL).

Bond angles (°)			
A(N2,N1,C5)	107.3827	A(N2,C23,C28)	121.1253
A(N2,N1,C34)	114.0398	A(C24,C23,C28)	120.1385
A(C5,N1,C34)	119.348	A(C23,C24,C25)	119.4982
A(N1,N2,C3)	109.5938	A(C23,C24,H29)	119.5256
A(N1,N2,C23)	119.1681	A(C25,C24,H29)	120.9663
A(C3,N2,C23)	123.8443	A(C24,C25,C26)	120.6918
A(N2,C3,C4)	104.3904	A(C24,C25,H30)	119.2412
A(N2,C3,O6)	124.9891	A(C26,C25,H30)	120.0653
A(C4,C3,O6)	130.5904	A(C25,C26,C27)	119.5084
A(C3,C4,C5)	108.4509	A(C25,C26,H31)	120.2561
A(C3,C4,N7)	118.1529	A(C27,C26,H31)	120.2351
A(C5,C4,N7)	133.314	A(C26,C27,C28)	120.4333
A(N1,C5,C4)	109.8282	A(C26,C27,H32)	120.1601
A(N1,C5,C38)	119.9292	A(C28,C27,H32)	119.4005
A(C4,C5,C38)	130.2421	A(C23,C28,C27)	119.7167
A(C4,N7,N8)	117.9326	A(C23,C28,H33)	119.7168
A(N7,N8,C9)	115.9037	A(C27,C28,H33)	120.5581
A(N8,C9,C10)	125.4225	A(N1,C34,H35)	111.1379
A(N8,C9,C14)	116.4365	A(N1,C34,H36)	109.1582
A(C10,C9,C14)	118.1407	A(N1,C34,H37)	108.7584
A(C9,C10,C11)	119.5431	A(H35,C34,H36)	109.3433
A(C9,C10,O15)	122.1014	A(H35,C34,H37)	109.8082
A(C11,C10,O15)	118.3555	A(H36,C34,H37)	108.5901
A(C10,C11,C12)	121.1588	A(C5,C38,H39)	111.1438
A(C10,C11,H20)	117.9236	A(C5,C38,H40)	111.143
A(C12,C11,H20)	120.9171	A(C5,C38,H41)	109.2703
A(C11,C12,C13)	119.53	A(H39,C38,H40)	108.3535
A(C11,C12,N17)	120.455	A(H39,C38,H41)	106.9915
A(C13,C12,N17)	119.973	A(H40,C38,H41)	109.8451
A(C12,C13,C14)	119.5561		
A(C12,C13,H21)	119.8419		
A(C14,C13,H21)	120.6013		
A(C9,C14,C13)	122.071		
A(C9,C14,H22)	117.3025		
A(C13,C14,H22)	120.6265		
A(C10,O15,H16)	107.3641		
A(C12,N17,H18)	117.4924		
A(C12,N17,H19)	117.5924		
A(H18,N17,H19)	114.2606		
A(N2,C23,C24)	118.7342		

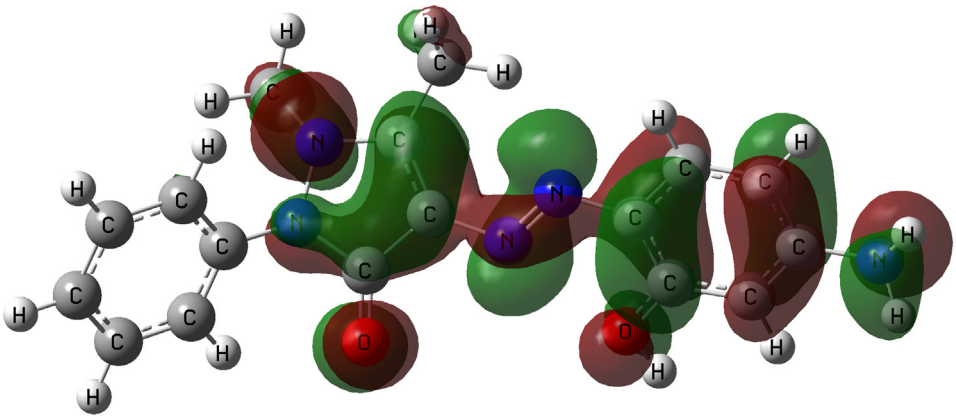

HOMO

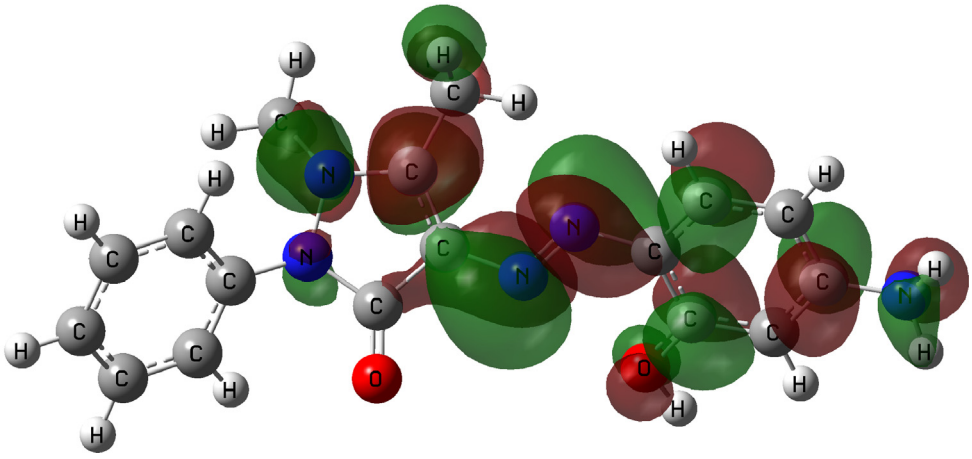

LUMO

Fig. 4. HOMO and LUMO molecular orbitals of ligand (HL).

Table 3
The calculated quantum chemical parameters of the ligand (HL).

Parameter	
E_{HOMO} (a.u.)	−0.19739
E_{LUMO} (a.u.)	−0.06899
μ (D)	4.529
T.E (a.u)	−1082.473
ΔE (a.u.)	0.1284
χ (a.u.)	0.1331
η (a.u.)	0.0642
σ (a.u.)$^{-1}$	15.578
Pi (a.u.)	−0.1331
S (a.u.)$^{-1}$	7.7888
ω (a.u.)	0.1379
ΔN_{max}	2.074

$$\omega = \frac{Pi^2}{2\eta} \tag{7}$$

$$\Delta N_{max} = -\frac{Pi}{\eta}. \tag{8}$$

The HOMO–LUMO energy gap, ΔE, which is an important stability index, is applied to develop theoretical models for explaining the structure and conformation barriers in many molecular systems. Recently, the energy gap has been used to prove the reactivity and stability of the compounds [3,12]. The dipole moment, μ, the first derivative of the energy with respect to an applied electric field, was used to discuss and rationalize the structure [3,12].

Table 4
Energy values obtained in docking calculations of ligand (HL) with receptor prostate cancer mutant 2q2k and breast cancer mutant 3hb5.

Receptor	Est. free energy of binding (kcal/mol)	Est. inhibition constant (K_i) (μM)	vdW + bond + desolv energy (kcal/mol)	Electrostatic energy (kcal/mol)	Total intercooled energy (kcal/mol)	Interact surface
2q2k	−2.99	6.40	−4.90	+0.07	−4.83	492.401
3hb5	−3.60	2.28	−4.63	−0.02	−4.65	506.328

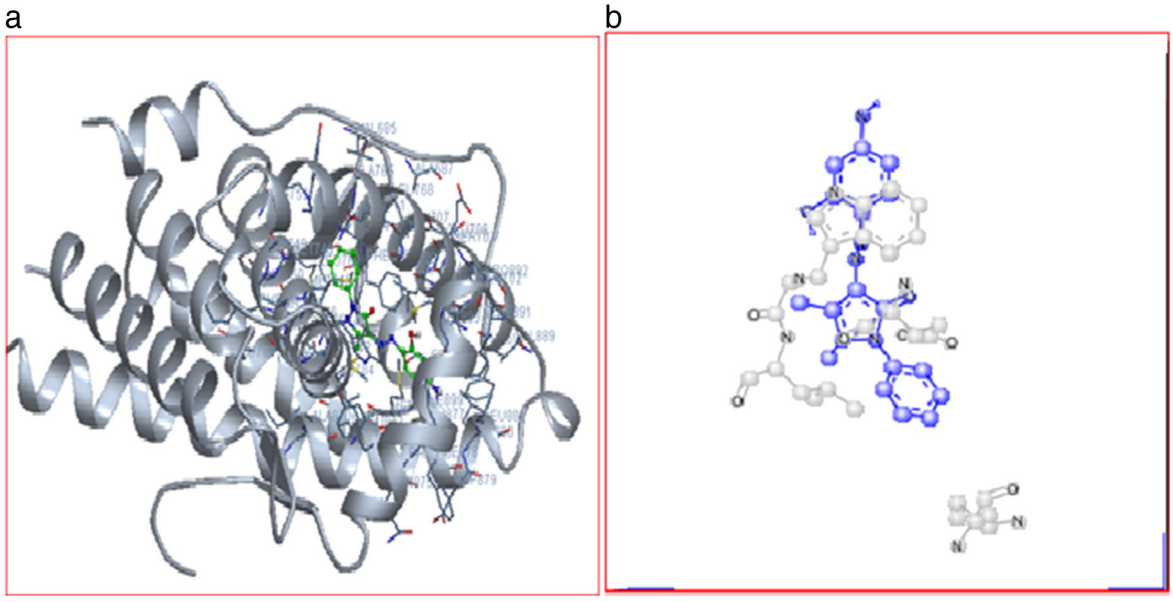

Fig. 5. Fig. 5. The ligand (HL) (green in (A) and blue in (B)) in interaction with receptor prostate cancer mutant 2q2k. (For interpretation of the references to color in this figure legend, the reader is referred to the web version of this article).

3.3. Molecular docking

Cancer can be described as the uncontrolled growth of abnormal cells. Prostate cancer is the most common non-skin malignancy in men. Except for lung cancer, it is responsible for more deaths than any other cancer. The American Cancer Society (ACS) estimated 1 man in 6 will be diagnosed with prostate cancer during his lifetime. A little over 1.8 million men in the United States are survivors of prostate cancer [23].

Breast cancer is one of the most recurring worldwide diagnosed and deadliest cancers next to lung cancer with a high number of mortality rates among females [24]. At global level, it accounted for more than 1.6 million new cases in 2010. The incidence or prevalence rate of the breast cancer in India is expected to be more than 90,000 in the coming years and over 50,000 women die each year.

Molecular docking is a key tool in computer drug design [25]. The focus of molecular docking is to simulate the molecular recognition process. Molecular docking aims to achieve an optimized conformation for both the protein and drug with relative orientation between them such that the free energy of the overall system is minimized.

In this context, we used molecular docking between ligand (HL) and prostate cancer mutant 2q2k-Hormone and breast cancer (3hb5). The results showed a possible arrangement between ligand (HL) and receptor (2q2k, 3hb5). The docking study showed a favorable interaction between ligand (HL) and the receptor (2q2k, 3hb5) and the calculated energy is listed in Table 4 and Figs. 5(a, b) and 6(a_1, b_1) for receptors

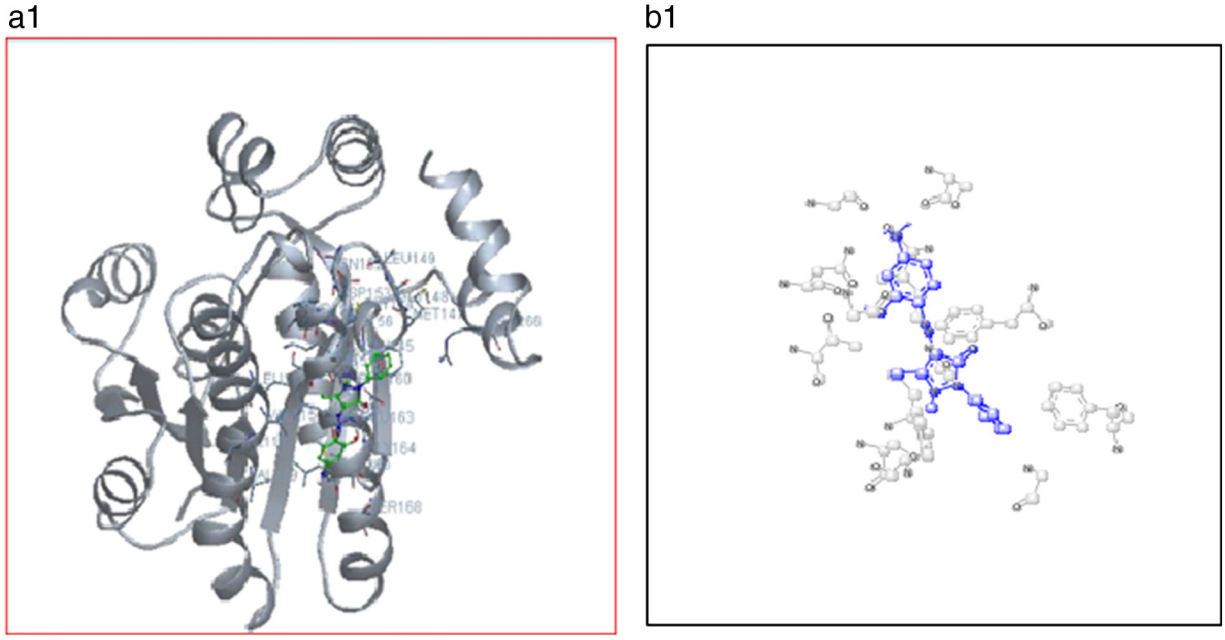

Fig. 6. The ligand (HL) (green in (a1) and blue in (b1)) in interaction with receptor breast cancer mutant 3hb5. (For interpretation of the references to color in this figure legend, the reader is referred to the web version of this article).

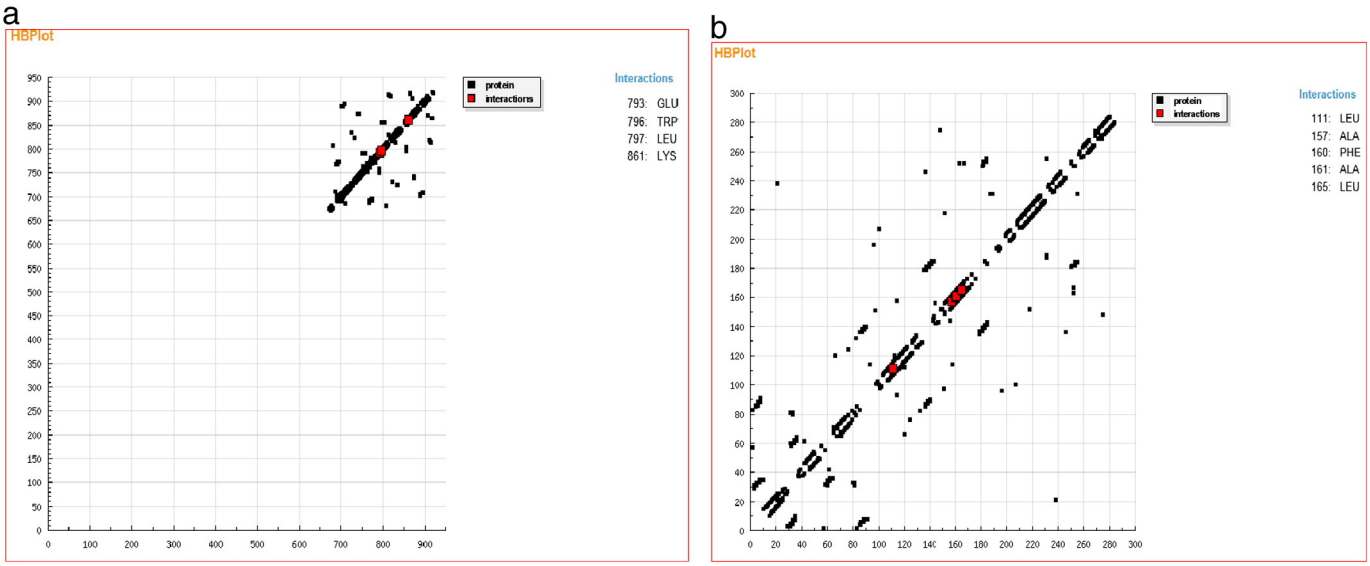

Fig. 7. HB plot of interaction between ligand (HL) with receptor a) prostate cancer mutant 2q2k and b) breast cancer mutant 3hb5.

2q2k and 3hb5, respectively. According to the results obtained in this study, HB plot curve indicates that, the ligand (HL) binds to the two proteins with hydrogen bond interactions and decomposed interaction energies in kcal/mol exist between the of ligand (HL) and receptors (2q2k and 3hb5) as shown in Fig. 7. The calculated efficiency is favorable where K_i values estimated by AutoDock were compared with experimental K_i values, when available, and the Gibbs free energy is negative. Also, based on this data, we can propose that interaction between the 2q2k and 3hb5 receptors and the ligand (HL) is possible. 2D plot curves of docking with ligand (HL) are shown in Fig. 8. This interaction could activate apoptosis in cancer cell energy of interactions with ligand (HL). Binding energies are most widely used as a mode of measuring binding affinity of a ligand. Thus, a decrease in binding energy due to mutation will increase the binding affinity of the azo dye ligand towards the receptor. The characteristic feature of azodye ligand was represented in the presence of several active sites available for hydrogen bonding. This feature gives them the ability to be good binding inhibitors to the protein and will help to produce augmented inhibitory compounds.

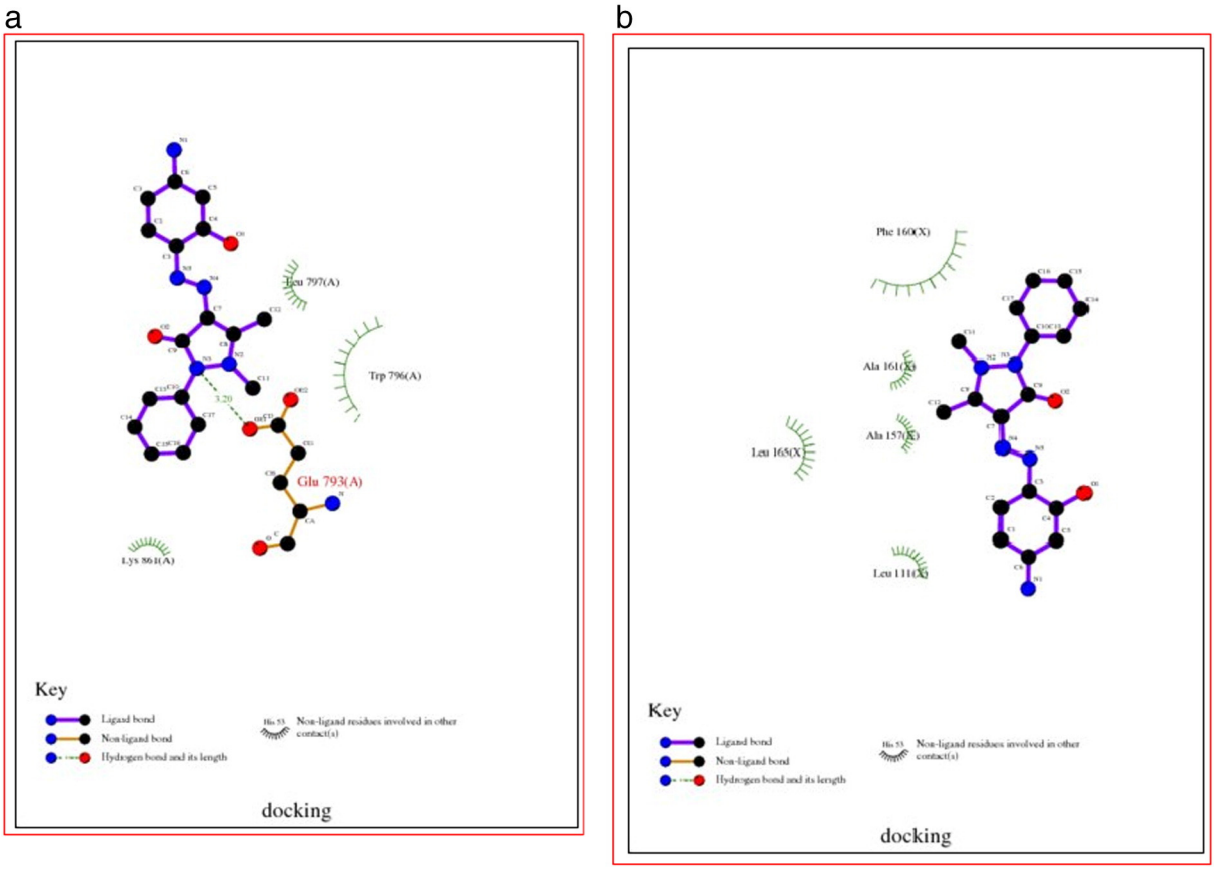

Fig. 8. 2D plot of interaction between ligand (HL) with receptor a) prostate cancer mutant 2q2k and b) breast cancer mutant 3hb5.

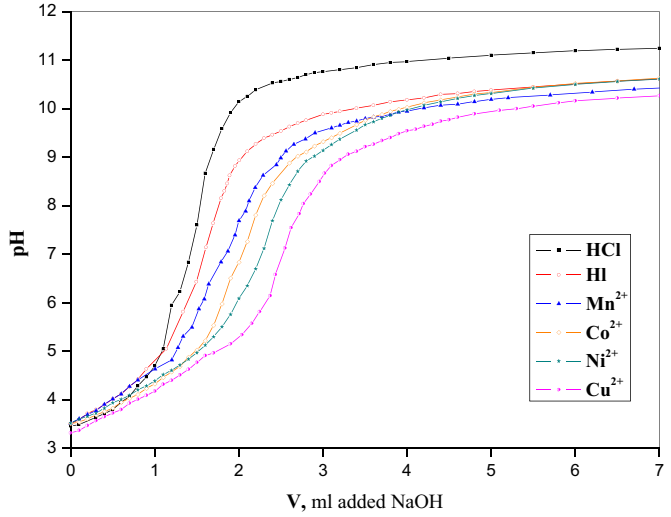

Fig. 9. Potentiometeric titration curves of HL ligand and its metal complexes.

The results confirmed also that, the azodye ligand derived from 3-amino phenol is an efficient inhibitor of prostate cancer mutant 2q2k-Hormone and breast cancer mutant 3hb5-Oxidoreductase.

3.4. Potentiometric studies

The interaction of a metal with an electron donor atom of a ligand (HL) is usually followed by the release of H^+ ions. Alkaline potentiometric titrations are based on the detection of the protons released upon complexation. The main advantage of this technique, compared to other methods is that from the titration curves it is possible to follow complexation continuously as a function of pH and to detect exactly at which pH complexation takes place. Furthermore, it is possible to calculate the dissociation constants and the stability constants from the potentiometric titration curves as shown in Fig. 9. The average number of the protons associated with HL ligand at different pH values, $\bar{n}_A$, was calculated from the titration curves of the acid in the absence and presence of ligand (HL) by applying Eq. (9):

$$\bar{n}_A = Y \pm \frac{(V_1 - V_2)(N^\circ + E^\circ)}{(V^\circ - V_1)TC^\circ_L} \tag{9}$$

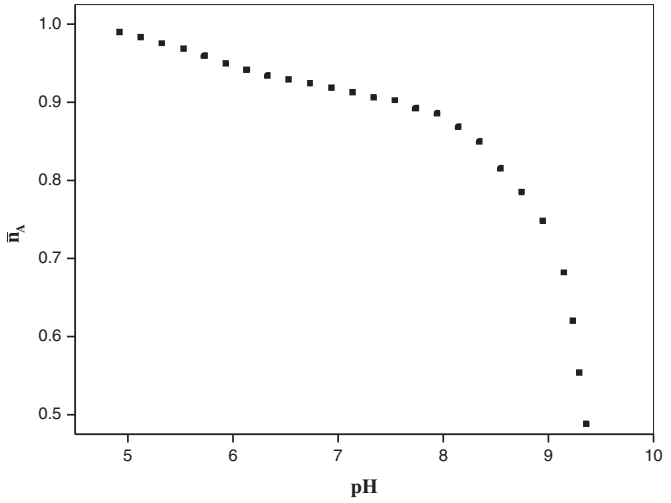

Fig. 10. The relation between $\bar{n}_A$ *vs.* pH for HL ligand.

Table 5
Thermodynamic functions for the dissociation of HL in 20% (by volume) DMF–water mixture in the presence of 0.1 M KCl at different temperatures.

Temperature (K)	Dissociation Constant (pK^H)	Free energy change (ΔG) (kJ mol^{-1})	Enthalpy change (ΔH) (kJ mol^{-1})	Entropy change (−ΔS) (J mol^{-1} K^{-1})
298	9.40	53.63	35.32	61.46
308	9.23	54.43		62.05
318	9.01	54.86		61.45

where Y is the number of available protons in HL ligand (Y = 1) and V_1 and V_2 are the volumes of alkali required to reach the same pH on the titration curve of hydrochloric acid and reagent, respectively, V° is the initial volume (50 cm^3) of the mixture, TC°_L is the total concentration of the reagent, N° is the normality of sodium hydroxide solution and E° is the initial concentration of the free acid. Thus, the formation curves ($\bar{n}_A$ *vs.* pH) for the proton–ligand systems were constructed and found to extend between 0 and 1 in the $\bar{n}_A$ scale shown in Fig. 10. This means that azo of 3-aminophenol has one ionizable proton. Different computational methods were applied to evaluate the dissociation constant [26]. Three replicate titrations were performed and the average values obtained are listed in Table 5. The completely protonated form of ligand (HL) has one dissociable proton, that dissociates in the measurable pH range.

The formation curves for the metal complexes were obtained by plotting the average number of ligand attached per metal ion ($\bar{n}_A$) *vs.* the free ligand exponent (pL), according to Irving and Rossotti [27]. The average number of the reagent molecules attached per metal ion, $\bar{n}_A$, and free ligand exponent, pL, can be calculated using Eqs. (10) and (11):

$$\bar{n} = \frac{(V_3 - V_2)(N^\circ + E^\circ)}{(V^\circ - V_2)\cdot \bar{n}_A \cdot TC^\circ_M} \tag{10}$$

and

$$pL = \log_{10} \frac{\sum_{n=o}^{n=J} \beta^H_n \left(\frac{1}{[H^+]}\right)^n}{TC^\circ_L - \bar{n}\cdot TC^\circ_M} \cdot \frac{V^o + V_3}{V^o} \tag{11}$$

where TC°_M is the total concentration of the metal ion present in the solution, and β^H_n is the overall proton-reagent stability constant. V_1, V_2 and V_3 are the volumes of alkali required to reach the same pH on the titration curves of hydrochloric acid, organic ligand and complex, respectively. These curves were analyzed and the successive metal–ligand stability constants were determined using different computational methods [28,29]. The values of the stability constants (log K_1 and log K_2) are given in Table 6. The following general remarks can be pointed out:(i) The maximum value of $\bar{n}$ was ~2 indicating the formation of 1:1 and 1:2 (metal:ligand) complexes only [2,3].(ii) The metal ion solution used in the present study was very dilute (2×10^{-4} M), hence there was no possibility of the formation of polynuclear complexes [30,31].(iii) The metal titration curves were displaced to the right-hand side of the ligand titration curves along the volume axis, indicating

Table 6
Stepwise stability constants for ML and ML_2 complexes of HL in 20% (by volume) DMF–water mixture in the presence of 0.1 M KCl at different temperatures.

M^{n+}	298 K		308 K		318 K	
	log K_1	log K_2	log K_1	log K_2	log K_1	log K_2
Mn(II)	5.49	4.41	5.63	4.52	5.74	4.61
Co(II)	5.57	4.50	5.72	4.64	5.82	4.76
Ni(II)	5.67	4.63	5.80	4.75	5.93	4.85
Cu(II)	5.81	4.70	5.93	4.83	6.01	4.95

proton release upon complex formation of the metal ion with the ligand. The large decrease in pH for the metal titration curves relative to ligand titration curve points to the formation of strong metal complexes [32, 33].(iv) At constant temperature, the stability of the chelates increases in the order of Cu(II) > Ni(II) > Co(II) > Mn(II) [2,3]. This order largely reflects that the stability of Cu(II) complex is considerably larger than those of other metals of the 3d series. Under the influence of both the polarizing ability of the metal ion and the ligand field, Cu(II) complex will receive some extra stabilization due to tetragonal distortion of octahedral symmetry in its complexes. The greater stability of Cu(II) complex is produced by the well known Jahn–Teller effect [34].

Stepwise dissociation constants for the HL ligand and the stepwise stability constants of its complexes with Mn(II), Co(II), Ni(II) and Cu(II) ions have been calculated at 298, 308 and 318 K. The corresponding thermodynamic parameters (ΔG, ΔH and ΔS) were evaluated.

The dissociation constants (pK_a) for HL, as well as the stability constants of its complexes with Mn(II), Co(II), Ni(II) and Cu(II) ions have been evaluated at 298, 308 and 318 K and are given in Tables 5 and 6, respectively. The enthalpy (ΔH) for the dissociation and complexation process was calculated from the slope of the plot pK_a or log K *vs.* $^1/_T$ using the graphical representation of van't Hoff Eqs. (12) and (13):

$$\Delta G = -2.303\,RT\,\log K = \Delta H - T\Delta S \tag{12}$$

or

$$\log K = \left(\frac{-\Delta H}{2.303R}\right)\left(\frac{1}{T}\right) + \frac{\Delta S}{2.303R} \tag{13}$$

where R is the gas constant = 8.314 $J\cdot mol^{-1}\cdot K^{-1}$, K is the dissociation constant for the ligand stability and T is the temperature (K).

The values of free energy change (ΔG) and enthalpy (ΔH), can be deduced the entropy (ΔS) using the well known relationships (12) and (14):

$$\Delta S = (\Delta H - \Delta G)/T. \tag{14}$$

The thermodynamic parameters of the dissociation process of HL are recorded in Table 5. From these results the following points can be made:

(i) The pK_a values decrease with increasing temperature, i.e. the acidity of ligand increases [2,3].
(ii) Positive values of ΔH indicate that dissociation is accompanied by absorption of heat and the process is endothermic.
(iii) Large positive values of ΔG indicate that the dissociation process is not spontaneous [2,35].
(iv) Negative values of ΔS are due to increased order as the result of the solvation processes.

Table 7
Thermodynamic functions for ML and ML_2 complexes of HL in 20% (by volume) DMF–water mixture and 0.1 M KCl.

M(II)	T (K)	Free energy change (kJ mol^{-1})		Enthalpy change (kJ mol^{-1})		Entropy change (J mol^{-1} K^{-1})	
		$-\Delta G_1$	$-\Delta G_2$	ΔH_1	ΔH_2	ΔS_1	ΔS_2
Mn(II)	298	31.32	25.16	22.70	18.16	181.29	145.37
	308	33.20	26.66			181.51	145.49
	318	34.95	28.07			181.29	145.37
Co(II)	298	31.78	25.67	22.72	23.60	182.89	165.35
	308	33.73	27.36			183.29	165.46
	318	35.44	28.98			182.89	165.35
Ni(II)	298	32.35	26.42	23.58	19.97	187.69	155.67
	308	34.21	28.01			187.61	155.79
	318	36.11	29.53			187.69	155.66
Cu(II)	298	34.29	33.16	18.181	22.68	176.07	187.36
	308	36.27	34.97			176.77	187.18
	318	38.91	36.59			179.51	186.41

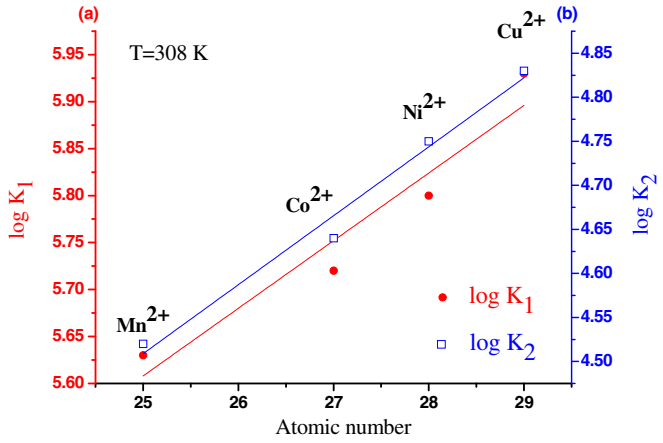

Fig. 11. The relation between stability constants (log K_1 and log K_2) and atomic number of metal complexes.

All the thermodynamic parameters of stepwise stability constants for the complexes of ligand (HL) are recorded in Table 7. It is known that the divalent metal ions exist in solution as octahedral hydrated species [3,35] and the obtained values ΔH and ΔS can then be considered as the sum of two contributions: (a) release of H_2O molecules and (b) metal–ligand bond formation. Examination of these values shows that:

(i) The stability constants (log K_1 and log K_2) for the rhodanine azodye complexes increase with increasing temperature [3,35].
(ii) The stability constants of Mn(II), Co(II), Ni(II) and Cu(II) complexes were increased with increasing atomic number in the order of Cu(II) > Ni(II) > Co(II) > Mn(II) at constant temperature as shown in Fig. 11.
(iii) The negative values of ΔG for the complex formation suggest a spontaneous nature of such process [2].
(iv) The positive values of ΔH mean that the complex formation processes is endothermic and favored at higher temperature.
(v) The positive values of ΔS confirm that the complex formation processes are entropically favorable [2,3].

4. Conclusion

The proton–ligand dissociation constant of 4-(2,3-dimethyl-1-phenylpyrazol-5-one azo)-3-aminophenol (HL) and metal–ligand stability constants of its complexes with metal ions (Mn(II), Co(II), Ni(II) and Cu(II)) at different temperatures were determined. At constant temperature the stability constants of the formed complexes decrease in the order of Cu(II), Ni(II), Co(II) and Mn(II). The dissociation process is non-spontaneous, endothermic and entropically unfavorable. The formation of the metal complexes has been found to be spontaneous, endothermic and entropically favorable. The values of stability constants (log K_1 and log K_2) of rhodanine azodye complexes increase with increasing temperature.

References

[1] Z. Seferoglu, N. Ertan, Russ. J. Org. Chem. 43 (2007) 1035–1041.
[2] A.A. El-Bindary, A.Z. El-Sonbati, M.A. Diab, Sh.M. Morgan, J. Mol. Liq. 201 (2015) 36–42.
[3] A.Z. El-Sonbati, A.A. El-Bindary, S.A. Abd El-Meksoud, A.A.M. Belal, R.A. El-Boz, J. Mol. Liq. 199 (2014) 538–544.
[4] A.Z. El-Sonbati, M.A. Diab, A.A. El-Bindary, Sh.M. Morgan, Inorg. Chim. Acta 404 (2013) 175–187.
[5] M.A. Diab, A.Z. El-Sonbati, A.A. El-Bindary, G.G. Mohamed, Sh.M. Morgan, Res. Chem. Intermed. (2015). http://dx.doi.org/10.1007/s11164-015-1946-0.

[6] K. Georgiadou, E.G. Tsatsaroni, Dyes Pigm. 53 (2002) 73–78.
[7] A.Z. El-Sonbati, M.A. Diab, A.A. El-Bindary, A.M. Eldesoky, Sh.M. Morgan, Spectrochim. Acta A 135 (2015) 774–791.
[8] E. Yuriev, M. Agostino, P.A. Ramsland, J. Mol. Recognit. 24 (2011) 149–164.
[9] T. Cheng, Q. Li, Z. Zhou, Y. Wang, S. Bryant, AAPS J. 14 (2012) 133–141.
[10] N.A. El-Ghamaz, A.Z. El-Sonbati, M.A. Diab, A.A. El-Bindary, G.G. Mohamed, Sh.M. Morgan, Spectrochim. Acta A 147 (2015) 200–211.
[11] G.H. Jeffery, J. Bassett, J. Mendham, R.C. Deney, Vogel's Textbook of Quantitative Chemical Analysis, 5th edition Longman, London, 1989.
[12] A.A. El-Bindary, A.Z. El-Sonbati, M.A. Diab, E.E. El-Katori, H.A. Seyam, Int. J. Adv. Res. Comput. Sci. 2 (2014) 493–502.
[13] A.A. El-Bindary, A.Z. El-Sonbati, M.A. Diab, M.K. Abd El-Kader, J. Chem. 2013 (2013) (ID: 682186).
[14] A.A. Al-Sarawy, A.A. El-Bindary, A.Z. El-Sonbati, M.M. Mokpel, Pol. J. Chem. 80 (2006) 289–295.
[15] A.Z. El-Sonbati, A.A. El-Bindary, R.M. Ahmed, J. Solut. Chem. 32 (2003) 617–623.
[16] M.A. Quraishi, R. Sardar, D. Jamal, Mater. Chem. Phys. 71 (2001) 309–313.
[17] N.A. El-Ghamaz, A.Z. El-Sonbati, M.A. Diab, A.A. El-Bindary, M.K. Awad, Sh.M. Morgan, Mater. Sci. Semicond. Process. 19 (2014) 150–162.
[18] Z. Bikadi, E. Hazai, J. Chem. Inf. 11 (2009) 1–15.
[19] T.A. Halgren, J. Comput. Chem. 17 (1998) 490–519.
[20] G.M. Morris, D.S. Goodsell, J. Comput. Chem. 19 (1998) 1639–1662.
[21] R.G. Bates, M. Paabo, R.A. Robinson, J. Phys. Chem. 67 (1963) 1833–1838.
[22] H.M. Irving, M.G. Miles, L.D. Pettit, Anal. Chim. Acta 38 (1967) 475–488.
[23] G.A. American Cancer Society, Cancer Facts & Figures, American Cancer Society, Atlanta, 2014.
[24] J.R. Benson, I. Jatoi, Future Oncol. 8 (2012) 697–702.
[25] A. Beteringhe, C. Racuciu, C. Balan, E. Stoican, L. Patron, Adv. Mater. Res. 787 (2013) 236–240.
[26] H. Irving, H.S. Rossotti, J. Chem. Soc. 76 (1954) 2904–2910.
[27] H. Irving, H.S. Rossotti, J. Chem. Soc. 74 (1953) 3397–3405.
[28] F.J.C. Rossotti, H.S. Rossotti, Acta Chem. Scand. 9 (1955) 1166–1176.
[29] M.T. Beck, I. Nagybal, Chemistry of Complex Equilibrium, Wiley, New York, 1990.
[30] P. Sanyal, G.P. Sengupta, J. Indian Chem. Soc. 67 (1990) 342–344.
[31] S. Sridhar, P. Kulanthaip, P. Thillaiarasu, V. Thanikachalam, G.J. Manikandan, World J. Chem. 4 (2009) 133–140.
[32] V.D. Athawale, V.J. Lele, J. Chem. Eng. Data 41 (1996) 1015–1019.
[33] V.D. Athawale, S.S. Nerkar, Monatsh. Chem. 131 (2000) 267–276.
[34] L.E. Orgel, An Introduction to Transition Metal Chemistry Ligand Field Theory, Methuen, London, 1966. 55.
[35] A.F. Shoair, A.R. El-Shobaky, E.A. Azab, J. Mol. Liq. 203 (2015) 59–65.